

On rotated time-frequency kernels

Martin J. Bastiaans,¹ Tatiana Alieva,² and LJubiša Stanković³

Abstract—The principal axes of the time-frequency representation of a signal are defined as those mutually orthogonal directions in the time-frequency plane for which the width of the signal’s fractional power spectrum is minimum or maximum. The time-frequency kernels used in the Cohen class of time-frequency representations are then rotated in the time-frequency plane, in order to align the kernels’ preferred axes to the signal’s principal axes. It is shown that the resulting time-frequency representations show a better reduction of cross-terms without too severely degrading the auto-terms than the corresponding, original time-frequency representations.

Keywords—Wigner distribution, ambiguity function, fractional Fourier transform, time-frequency signal analysis

I. INTRODUCTION

TO represent a signal in a time-frequency plane, many time-frequency representations are used nowadays, each with its own advantages and disadvantages. The well-known Wigner distribution (WD) of a multi-component signal, for instance, shows highly concentrated auto-terms, but suffers from cross-terms, which may even hide some of the auto-terms. Many other distributions have been proposed to optimally represent the signal in a time-frequency plane, with significantly reduced cross-terms but without a too severe degrading of the auto-terms. Such distributions may result from a weighting of the WD by an appropriate time-frequency kernel, leading to Cohen’s class of time-frequency distributions.

In this paper we use kernels from the Cohen class, but we rotate these kernels in the time-frequency plane through an angle that is determined by the characteristics of the signal. In particular, we consider the signal’s fractional power spectrum – the squared modulus of the fractional Fourier transform – and find its principal axes, determined by those two orthogonal directions for which the width of the fractional power spectrum is minimum or maximum, respectively. We then show that if a kernel’s preferred axes are aligned to these two directions, the resulting time-frequency distribution shows a much better performance with respect to the auto-terms concentration and the cross-terms reduction, than the distribution that would have resulted if the original, non-aligned kernel would have been used. The more dominantly the time-frequency content of the signal is located along one principal axis, the better the improvement of the resulting time-frequency representation will be.

The authors are with ¹) Technische Universiteit Eindhoven, Faculteit Elektrotechniek, Postbus 513, 5600 MB Eindhoven, Netherlands (e-mail: m.j.bastiaans@tue.nl), ²) Universidad Complutense de Madrid, Facultad de Ciencias Físicas, 28040 Madrid, Spain (e-mail: talieva@fis.ucm.es), and ³) University of Montenegro, Elektrotehnicki fakultet, 81000 Podgorica, Montenegro, Yugoslavia (e-mail: l.stankovic@ieee.org).

The proposed procedure is demonstrated on a multi-component signal, using some of the well-known Cohen-class kernels.

II. WIGNER DISTRIBUTION AND THE COHEN CLASS

Let us start with the WD $W_x(t, f)$ of a time signal $x(t)$, defined as

$$W_x(t, f) = \int_{-\infty}^{\infty} x(t + \frac{1}{2}\tau)x^*(t - \frac{1}{2}\tau) \exp(-j2\pi f\tau) d\tau. \quad (1)$$

It is well known that the WD of a multicomponent signal suffers from cross-terms. Therefore, a weighted version of the WD is often used as a time-frequency representation of the signal, where the weighting kernel $\Phi(t, f)$ is chosen such that the cross-terms are reduced without degrading the auto-terms too severely. This leads to the Cohen class of time-frequency representations [1]:

$$C_x(t, f) = \int_{-\infty}^{\infty} \int_{-\infty}^{\infty} \Phi(t_o, f_o) W_x(t - t_o, f - f_o) dt_o df_o. \quad (2)$$

Many kernels have been proposed during the past decades [2].

In designing a kernel $\Phi(t, f)$, it is advantageous to go from the Wigner domain to the ambiguity domain by means of a Fourier/inverse Fourier transformation (FIFT). In that case, the FIFT $\bar{C}_x(\tau, \nu)$ of the time-frequency representation $C_x(t, f)$,

$$\bar{C}_x(\tau, \nu) = \int_{-\infty}^{\infty} \int_{-\infty}^{\infty} C_x(t, f) \exp[-j2\pi(\nu t - f\tau)] dt df, \quad (3)$$

is related to the FIFT $\bar{\Phi}(\tau, \nu)$ of the kernel $\Phi(t, f)$ and the ambiguity function (AF) $A_x(\tau, \nu)$,

$$A_x(\tau, \nu) = \int_{-\infty}^{\infty} x(t + \frac{1}{2}\tau)x^*(t - \frac{1}{2}\tau) \exp(-j2\pi\nu t) dt, \quad (4)$$

by a simple product relation:

$$\bar{C}_x(\tau, \nu) = \bar{\Phi}(\tau, \nu) A_x(\tau, \nu). \quad (5)$$

We remark that the AF is the FIFT of the WD,

$$A_x(\tau, \nu) = \int_{-\infty}^{\infty} \int_{-\infty}^{\infty} W_x(t, f) \exp[-j2\pi(\nu t - f\tau)] dt df, \quad (6)$$

and that the moments of the WD are related to the derivatives of the AF as

$$\begin{aligned} & \int_{-\infty}^{\infty} \int_{-\infty}^{\infty} W_x(t, f) t^n f^m dt df \\ &= \frac{(-1)^n}{(j2\pi)^{m+n}} \left. \frac{\partial^{m+n} A_x(\tau, \nu)}{\partial \tau^m \partial \nu^n} \right|_{\tau=\nu=0}. \end{aligned} \quad (7)$$

As examples of time-frequency kernels for some well-known time-frequency distributions, we mention [2]

- Wigner 1,
- Born-Jordan $\sin(\pi\tau\nu)/\pi\tau\nu,$
- Zhao-Atlas-Marks (cone) $g(\tau)|\tau| \sin(\pi\tau\nu)/\pi\tau\nu,$
- Butterworth $1/[1 + (\tau/\tau_o)^{2M}(\nu/\nu_o)^{2N}],$
- Choi-Williams (exponential) $\exp[-(2\pi\tau\nu)^2/\sigma],$
- generalized exponential $\exp[-(\tau/\tau_o)^{2M}(\nu/\nu_o)^{2N}],$

where the Choi-Williams kernel is a special case of the generalized exponential kernel with $M = N = 1$ and $\sigma = (2\pi\tau_o\nu_o)^2$.

In many cases the kernel $\Phi(t, f)$ [and $\bar{\Phi}(\tau, \nu)$] shows a preferred behaviour in the time and/or the frequency direction. The degree of cross-term reduction (and degrading of the auto-terms) then depends on the way in which the WD is oriented in the time-frequency plane. If the orientation is along the time and/or the frequency direction, the kernel may act as expected; in the case of a different orientation, the effect of the kernel is not optimal [3]. We therefore suggest to rotate the kernel in such a way that its preferred axes coincide with the principal axes of the WD (and the AF). Note that, although the rotated distributions may not satisfy the common marginal properties, they satisfy generalized ones [4].

III. FRACTIONAL FOURIER TRANSFORM

To find the principal axes of the WD (and the AF), we introduce the fractional Fourier transform (FT) $X_\alpha(u)$ of the signal $x(t)$, defined by [5]

$$X_\alpha(u) = \int_{-\infty}^{\infty} K_\alpha(t, u)x(t)dt, \quad (8)$$

where the kernel $K_\alpha(t, u)$ is given by

$$K_\alpha(t, u) = \frac{\exp(j\frac{1}{2}\alpha)}{\sqrt{j \sin \alpha}} \exp\left(j\pi \frac{(t^2 + u^2) \cos \alpha - 2ut}{\sin \alpha}\right). \quad (9)$$

Note that, in particular, $X_0(u) = x(u)$, $X_\pi(u) = x(-u)$, and that $X_{\pi/2}(u)$ corresponds to a normal FT.

It is well known (see for example [5], [6], or [7]) that the fractional FT corresponds to a rotation of the WD in the (t, f) plane, as well as to a rotation of the AF in the (τ, ν) plane:

$$W_{X_\alpha}(t, f) = W_x(t \cos \alpha - f \sin \alpha, t \sin \alpha + f \cos \alpha) \quad (10)$$

$$A_{X_\alpha}(\tau, \nu) = A_x(\tau \cos \alpha - \nu \sin \alpha, \tau \sin \alpha + \nu \cos \alpha). \quad (11)$$

If we introduce the fractional power spectra $|X_\alpha(t)|^2$ as the squared moduli of the corresponding fractional FTs, we have the following relations between these fractional power spectra on the one hand and the WD and the AF on the other:

$$|X_\alpha(t)|^2 = \int_{-\infty}^{\infty} W_{X_\alpha}(t, f)df, \quad (12)$$

$$|X_\alpha(t)|^2 = \int_{-\infty}^{\infty} A_{X_\alpha}(0, \nu) \exp(j2\pi\nu t) d\nu. \quad (13)$$

IV. MOMENTS OF THE FRACTIONAL POWER SPECTRA

We now introduce the moments of the fractional power spectra [8]. For the zero-order moment $E = \int_{-\infty}^{\infty} |X_\alpha(t)|^2 dt$ we have $E = \int_{-\infty}^{\infty} \int_{-\infty}^{\infty} W_{X_\alpha}(t, f) dt df = A_{X_\alpha}(0, 0)$ [see Eqs. (12) and (13), and also Eq. (7) with $m = n = 0$]. Note that the zero-order moment represents the signal's energy and that – in accordance with Parseval's theorem for a unitary transformation – it does not depend on α .

For the (normalized) first-order moments m_α , with $m_\alpha E = \int_{-\infty}^{\infty} |X_\alpha(t)|^2 t dt$, we may proceed along the same lines, now choosing $m = 0$ and $n = 1$ in Eq. (7). Note that the first-order moments are related to the centers of gravity of the fractional power spectra and that they satisfy the relationship $m_\alpha = m_0 \cos \alpha + m_{\pi/2} \sin \alpha$.

For the (normalized) second-order moments w_α , with $w_\alpha E = \int_{-\infty}^{\infty} |X_\alpha(t)|^2 t^2 dt$, we have

$$\begin{aligned} w_\alpha E &= \int_{-\infty}^{\infty} \int_{-\infty}^{\infty} W_{X_\alpha}(t, f) t^2 dt df \\ &= \frac{1}{(2\pi j)^2} \left. \frac{\partial^2 A_{X_\alpha}(0, \nu)}{\partial \nu^2} \right|_{\nu=0} \end{aligned} \quad (14)$$

[see Eq. (7) with $m = 0$ and $n = 2$]. We also introduce the *mixed* second-order moments of the WD and the *mixed* second-order derivative of the AF, while defining the (normalized) mixed second-order moments μ_α [see Eq. (7) with $m = n = 1$]:

$$\begin{aligned} \mu_\alpha E &= \frac{1}{4\pi j} \int_{-\infty}^{\infty} \left[\frac{\partial X_\alpha(t)}{\partial t} X_\alpha^*(t) - X_\alpha(t) \frac{\partial X_\alpha^*(t)}{\partial t} \right] t dt \\ &= \int_{-\infty}^{\infty} \int_{-\infty}^{\infty} W_{X_\alpha}(t, f) t f dt df \\ &= \frac{-1}{(2\pi j)^2} \left. \frac{\partial^2 A_{X_\alpha}(\tau, \nu)}{\partial \tau \partial \nu} \right|_{\tau=0, \nu=0}. \end{aligned} \quad (15)$$

We remark that instead of the second-order moments w_α and μ_α , we could as well consider the *central* second-order moments $w_\alpha - m_\alpha^2$ and $\mu_\alpha - m_\alpha m_{\alpha+\pi/2}$, which lead to similar expressions as the ones that we find for the normal moments. Note that the central second-order moments are related to the effective widths of the fractional power spectra.

The second-order moments satisfy the relationships

$$w_\alpha = w_0 \cos^2 \alpha + w_{\pi/2} \sin^2 \alpha + \mu_0 \sin 2\alpha, \quad (16)$$

$$\mu_\alpha = -\frac{1}{2}(w_0 - w_{\pi/2}) \sin 2\alpha + \mu_0 \cos 2\alpha. \quad (17)$$

In general, all second-order moments w_α and μ_α can be obtained from any three second-order moments w_α taken for three different angles α from the region $[0, \pi)$; we have, for instance, $\mu_0 = w_{\pi/4} - \frac{1}{2}(w_0 + w_{\pi/2})$. This implies that the corresponding three fractional power spectra define all second-order moments.

From Eq. (16) we conclude that the sum of the moments $w_\alpha + w_{\alpha+\pi/2}$ does not depend on α ,

$$w_\alpha + w_{\alpha+\pi/2} = w_0 + w_{\pi/2}, \quad (18)$$

and from Eq. (17) we conclude that

$$\mu_\alpha + \mu_{\alpha+\pi/2} = 0. \quad (19)$$

From Eq. (16) it is easy to see that the first derivative of w_α with respect to the angle α equals zero for $\alpha = \alpha_e$, where α_e satisfies the relationship

$$\tan 2\alpha_e = \frac{2\mu_0}{w_0 - w_{\pi/2}} = \frac{2w_{\pi/4} - (w_0 + w_{\pi/2})}{w_0 - w_{\pi/2}}. \quad (20)$$

From the invariance relationship (18) we conclude that α_e determines the domain with the smallest w_α , while $\alpha_e \pm \frac{1}{2}\pi$ corresponds to the domain with the largest w_α , or vice versa. Moreover, from Eqs. (17), (19), and (20) we also conclude that $\mu_{\alpha_e} = \mu_{\alpha_e \pm \pi/2} = 0$.

We now identify the direction α_e with one of the principal axes, and the direction $\alpha_e \pm \frac{1}{2}\pi$ with the other one. If $\Phi(t, f)$ denotes the time-frequency kernel that we use, the rotated version reads $\Phi(t \cos \alpha + f \sin \alpha, -t \sin \alpha + f \cos \alpha)$, and the general Cohen-class time-frequency representation takes the form

$$C_x(t, f) = \int_{-\infty}^{\infty} \int_{-\infty}^{\infty} W_x(t - t_o, f - f_o) \times \Phi(t_o \cos \alpha + f_o \sin \alpha, -t_o \sin \alpha + f_o \cos \alpha) dt_o df_o. \quad (21)$$

Note that we can also write

$$C_{X_\alpha}(t, f) = \int_{-\infty}^{\infty} \int_{-\infty}^{\infty} W_{X_\alpha}(t - t_o, f - f_o) \Phi(t_o, f_o) dt_o df_o. \quad (22)$$

V. EXAMPLES

As an example, consider the signal

$$x(t) = \exp[-(3t)^8] \{ \exp[j(192\pi t^2 - 8 \cos(4\pi t)/\pi)] + \exp[j(64\pi t^2 + 8 \cos(4\pi t)/\pi)] \}. \quad (23)$$

The values of the normalized central moments are $w_0 = 1$, $w_{\pi/2} = 1.38$, $w_{\pi/4} = 0.07$. From Eq. (20), we get $\alpha_e = 41^\circ$ or $\alpha_e = -49^\circ$. The second-order moment in the direction 41° is smaller than in any other direction: $w_{41^\circ} = 0.057$, while the second-order moment in the orthogonal direction is the largest: $w_{-49^\circ} = 2.01$.

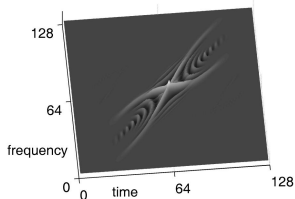


Fig. 1. Wigner distribution of the signal $x(t)$.

The WD of this signal has been depicted in Fig. 1. In Figs. 2-4 we have depicted the time-frequency representations that result from weighting this WD with several

kernels, both (a) without alignment and (b) with alignment of the kernels to the principal axes (41° and -49°) of the WD:

- Fig. 2: Butterworth, with $M = 1$ and $N = 3$,
 - Fig. 3: generalized exponential, with $M = 1$ and $N = 3$, and
 - Fig. 4: Zhao-Atlas-Marks (cone), with $g(\tau) = \cos^4(\pi\tau)$.
- The kernel parameters have been chosen such that for the signal under consideration the corresponding distributions show optimal results.

According to Eqs. (21) and (22), the three time-frequency distributions from the Cohen class are realized as a weighted WD, where the weighting kernel $\Phi(t, f)$ is the FIFT of $\bar{\Phi}(\tau, \nu)$. A region $-\frac{1}{2} \leq \tau < \frac{1}{2}$, $-128\pi \leq 2\pi\nu < 128\pi$ in the ambiguity domain is considered. This corresponds to the time interval $T = 1$ and the sampling interval $\Delta t = 1/128$. In discretization, 128 samples are taken along each ambiguity axis, and the two-dimensional inverse FIFT of the $\bar{\Phi}(\tau, \nu)$ -samples is calculated. The matrix $\Phi(n, k)$ obtained in this way is convolved with the WD, according to Eqs. (21) and (22), (original and rotated, respectively). The size of the obtained Cohen-class distribution is kept the same as the size of the WD, using the command `conv2(WD,Kernel,'same')` in MATLAB. The parameters τ_o , ν_o , M , and N for the Butterworth and the generalized exponential distribution are $\tau_o = 0.05$, $2\pi\nu_o = 25.6\pi$, $M = 1$, and $N = 3$, while the window $g(\tau)$ in the Zhao-Atlas-Marks distribution is a Hanning window: $g(\tau) = \cos^4(\pi\tau)$.

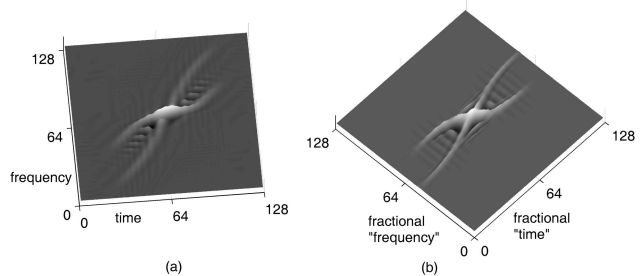


Fig. 2. Butterworth distribution of the signal $x(t)$ (a) without alignment and (b) with alignment of the kernel.

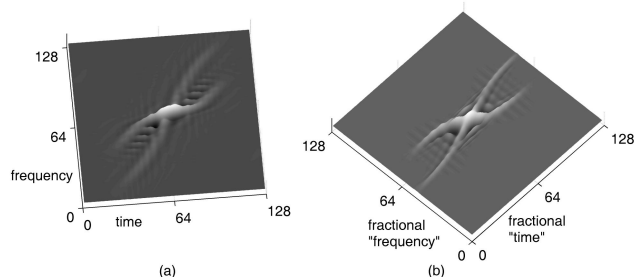


Fig. 3. Generalized exponential distribution of the signal $x(t)$ (a) without alignment and (b) with alignment of the kernel.

We conclude that the performance with respect to the auto-terms concentration and the cross-terms reduction, is better for the aligned kernels than for the non-aligned ones.

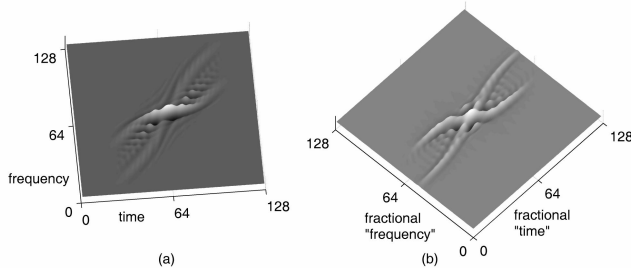


Fig. 4. Zhao-Atlas-Marks (cone kernel) distribution of the signal $x(t)$ (a) without alignment and (b) with alignment of the kernel.

Note that we have chosen kernels whose time-behaviour is significantly different from the frequency-behaviour; kernels that depend on the product $\tau\nu$ only – like the ones that lead to the Born-Jordan, the Choi-Williams (exponential), or the reduced interference distribution, for instance – do not show a clear improvement in cross-term reduction when they are rotated. Such kernels could be used, of course, after having been modified by an additional narrowing window in the τ -direction; cf. the Zhao-Atlas-Marks (cone) kernel, which differs from the Born-Jordan kernel by the additional window $g(\tau)|\tau|$.

We finally remark that we have considered the rotation of standard kernels. The same effect can be achieved by using standard kernels with an additional ambiguity domain axis corresponding to the determined principal axis, and generalized-marginal distributions [4]. Since, in this way, we introduce an additional rotated axis, the obtained results are very similar with the ones presented in this paper. These results will be presented in one of our next papers.

VI. CONCLUSION

The fractional power spectrum – i.e., the squared modulus of the fractional FT of a signal – is considered, and the signal's principal axes are defined as the two orthogonal directions for which the fractional power spectrum has a minimum or maximum width. A Cohen-class kernel that is used to smooth the WD, is then rotated in the time-frequency plane and oriented such that its preferred axes are aligned to these two directions. It is shown that the resulting time-frequency distribution yields a better cross-term reduction (without a too severe degrading of the auto-terms) than the corresponding, original distribution.

The better the signal is located along one principal axis, the better the improvement of the resulting time-frequency distribution will be. In the case that there is no clear principal direction, or there is more than one such direction, the procedure described might not yield a clear improvement. The case of multiple principal directions will be a subject for future work.

The method of aligning kernels to the signal's principal axes can be applied to rather arbitrary time-frequency representations. In a forthcoming paper we will demonstrate its effect on the weighting of the WD using the generalized [9] S-method [10], in which case the kernels in the

ambiguity domain and the Wigner domain are given by

$$\bar{\Phi}(\tau, \nu) = \int_{-\infty}^{\infty} A_{\gamma}(-\tau + \theta \sin \alpha, -\nu + \theta \cos \alpha) z(\theta) d\theta, \quad (24)$$

$$\Phi(t, f) = W_{\gamma}(-t, -f) Z(-[t \cos \alpha - f \sin \alpha]), \quad (25)$$

respectively, where $Z(f)$ is the FT of $z(t)$.

ACKNOWLEDGEMENT

T. Alieva would like to thank the Spanish Ministry of Education, Culture and Sports for financial help under contract SB 2000-0166. The work of L.J. Stanković is supported by the Volkswagen Stiftung, Germany.

REFERENCES

- [1] L. Cohen, *Time-Frequency Signal Analysis*. Englewood Cliffs, NJ: Prentice-Hall, 1995.
- [2] F. Hlawatsch and G. F. Boudreaux-Bartels, "Linear and quadratic time-frequency signal representations," *IEEE Signal Process. Mag.*, vol. **9**, nr. 2, April 1992, pp. 21–67.
- [3] A. K. Özdemir and O. Arikan, "A high resolution time frequency representation with significantly reduced cross-terms," *Proc. 2000 IEEE International Conference on Acoustics, Speech, and Signal Processing, ICASSP '00*, vol. **2**, pp. II693–II696, 2000.
- [4] X.-G. Xia, Y. Owechko, B. H. Soffer, and R. M. Matic, "On generalized-marginal time-frequency distributions," *IEEE Trans. Signal Process.*, vol. **44**, pp. 2882–2886, 1996.
- [5] L. B. Almeida, "The fractional Fourier transform and time-frequency representations," *IEEE Trans. Signal Process.*, vol. **42**, pp. 3084–3091, 1994.
- [6] A. W. Lohmann and B. H. Soffer, "Relationships between the Radon-Wigner and fractional Fourier transforms," *J. Opt. Soc. Am. A*, vol. **11**, pp. 1798–1801, 1994.
- [7] L.J. Stanković and I. Djurović, "Relationship between the Ambiguity function coordinate transformations and the fractional Fourier transform," *Annales des Télécommunications* vol. **53**, pp. 316–319, 1998.
- [8] T. Alieva and M. J. Bastiaans, "On fractional Fourier transform moments," *IEEE Signal Process. Lett.*, vol. **7**, pp. 320–323, 2000.
- [9] L.J. Stanković, T. Alieva, and M. J. Bastiaans, "Fractional-Fourier-domain Wigner distribution," *Proc. SSP 2001, 11th IEEE Signal Processing Workshop on Statistical Signal Processing*, ISBN 0-7803-7011-2, Institute of Electrical and Electronics Engineers, Piscataway, NJ, pp. 321–324, 2001.
- [10] L.J. Stanković, "A method for time-frequency signal analysis," *IEEE Trans. Signal Process.*, vol. **49**, pp. 225–229, 1994.